Borane B−C Bond Cleavage by a Low-Coordinate Iron Hydride Complex and N−N Bond Cleavage by the Hydridoborate Product

Ying Yu, William W. Brennessel, and Patrick L. Holland*

Department of Chemistry, University of Rochester, Rochester, New York 14627

Received April 19, 2007

The iron(II) hydride dimers [$L^RFe(\mu\text{-}H)_2FeL^R$] ($L^{Me}$ = 2,4-bis(2,6-diisopropylphenylimino)pent-3-yl; L^{tBu} = 2,2,6,6-tetramethyl-3,5-bis(2,6-diisopropylphenylimino)hept-4-yl) abstract hydrocarbyl groups from BR'_3 (R′ = Et, Ph) to give L^RFeR' and $L^RFe(\mu\text{-}H)_2BR'_2$. Mechanistic studies with R = R′ = Me are consistent with a process in which the hyride dimer opens one Fe−H bond, and subsequent B−H bond formation is concerted with dissociation of an Fe−H unit. Cleavage of boron−carbon bonds is likely to proceed at least in part from transient quaternary borate anions formed through disproportionation of $HBEt_3^-$. In a separate bond-breaking reaction, $L^{Me}Fe(\mu\text{-}H)_2BEt_2$ reacts with N_2H_4 to form a 1:1 adduct, which has been crystallographically characterized. Upon heating, it ejects H_2 from the bridging hydrides and cleaves the N−N bond to form the diaminoborate complex $L^{Me}Fe(\mu\text{-}NH_2)_2BEt_2$. These novel bond-breaking reactions are facilitated by the low coordination number at the iron(II) center.

Introduction

In addition to their classic roles as intermediates in homogeneous catalytic reactions of organometallic complexes,[1] iron hydrides have been postulated to be reactive intermediates in the mechanisms of hydrogenase[2] and nitrogenase[3] enzymes. We have become especially interested in exploring the chemistry of unsaturated hydride complexes of the late transition metals because of the juxtaposition of the reactive M−H functionality and an open coordination site for substrate binding.

We have used bulky β-diketiminate ligands (Figure 1) to enable the synthesis of the only known three- and four-coordinate iron hydride complexes.[4,5] These unsaturated iron hydrides, $L^RFe(\mu\text{-}H)_2FeL^R$, are prepared from reactions between iron(II) chloride complexes and potassium triethylborohydride (eqs 1 and 2).

$$[L^{Me}FeCl]_2 + 2KHBEt_3 \rightarrow L^{Me}Fe(\mu\text{-}H)_2FeL^{Me}\ (\mathbf{1a}) + 2\ BEt_3 + 2\ KCl \quad (1)$$

$$L^{tBu}FeCl + KHBEt_3 \rightarrow 0.5\ L^{tBu}Fe(\mu\text{-}H)_2FeL^{tBu}\ (\mathbf{1b}) + BEt_3 + KCl \quad (2)$$

Although both iron hydride compounds exist as dimers in the solid state, they behave differently in solution: $L^{tBu}Fe(\mu\text{-}H)_2FeL^{tBu}$ dissociates into monomers in solution,[4a] while only the dimer is observed in solutions of $L^{Me}Fe(\mu\text{-}H)_2FeL^{Me}$.[4b] One phenomenon caught our attention during the preparation of the iron hydride complexes: long reaction time (>30 min at room temperature) or heating leads to the formation of red products instead of the brown iron hydride complexes. Here, we report that the iron hydride complex reacts with the byproduct BEt_3 to give an iron dihydridoborate complex and an iron ethyl complex (Scheme 1).

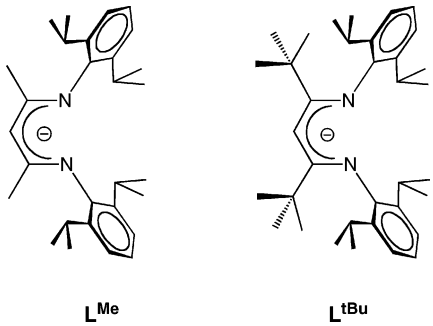

Figure 1. Diketiminate ligands L^R, where R indicates the substituent on the N_2C_3 backbone.

The reaction in Scheme 1 features migration of a boron-bound hydrocarbyl group. Boron-to-carbon migrations have precedent in the organic chemistry literature, where alkylboranes have been utilized for forming N−C or C−C bonds to nucleophiles that contain a potential leaving group (e.g., deprotonated α-haloesters or carbon monoxide).[6] In these reactions, trialkylborane initially attacks the nucleophile to form a quaternary adduct, and one of the boron R groups subsequently migrates to the adjacent N or C, displacing a leaving group. The migration of hydrocarbyl

* Corresponding author. E-mail: holland@chem.rochester.edu.

(1) (a) *Transition Metal Hydrides*; Dedieu, A., Ed.; VCH: New York, 1992. (b) *Recent Advances in Hydride Chemistry*; Peruzzini, M., Poli, R., Eds.; Elsevier: Amsterdam, 2001.

(2) Maroney, M. J. Hydrogen Metabolism and Hydrogenase. In *Biological Inorganic Chemistry*; Bertini, I., Gray, H. B., Stiefel, E. I., Valentine, J. S., Eds.; University Science Books: Sausalito, CA, 2007; pp 443−452.

(3) (a) Igarashi, R. Y.; Laryukhin, M.; Dos Santos, P. C.; Lee, H.-I.; Dean, D. R.; Seefeldt, L. C.; Hoffman, B. M. *J. Am. Chem. Soc.* **2005**, *127*, 6231−6241. (b) Lukoyanov, D.; Barney, B. M.; Dean, D. R.; Seefeldt, L. C.; Hoffman, B. M. *Proc. Natl. Acad. Sci. U.S.A.* **2007**, *104*, 1451−1455.

(4) (a) Smith, J. M.; Lachicotte, R. J.; Holland, P. L. *J. Am. Chem. Soc.* **2003**, *125*, 15752−15753. (b) Vela, J.; Smith, J. M.; Yu, Y.; Ketterer, N. A.; Flaschenriem, C. J.; Lachicotte, R. J.; Holland, P. L. *J. Am. Chem. Soc.* **2005**, *127*, 7857−7870.

(5) A four-coordinate iron(II) hydride complex has been implicated in the formation of a cyclohexadienyliron(II) complex: Brown, S. D.; Peters, J. C. *J. Am. Chem. Soc.* **2004**, *126*, 4538−4539. This insertion is analogous to the benzene reactivity of an isolated iron(II) silyl complex: Turculet, L.; Feldman, J. D.; Tilley, T. D. *Organometallics* **2003**, *22*, 4627−4629.

(6) Carey, R. A.; Sundberg, R. J. *Advanced Organic Chemistry, Part B: Reactions and Synthesis*, 4th ed.; Kluwer Academic/Plenum Publishers: New York, 2001; pp 549−563.

10.1021/om7003805 CCC: $37.00
Publication on Web 05/26/2007

Scheme 1

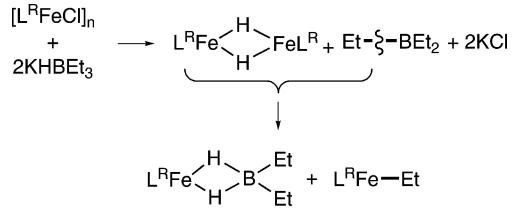

Scheme 2

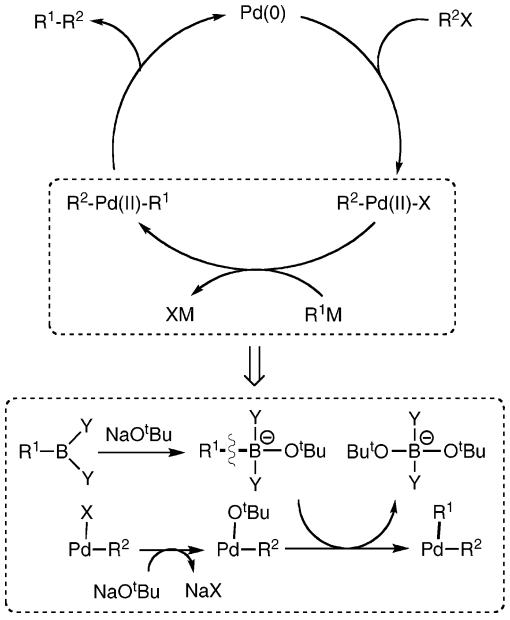

groups from boron to a transition metal is also a key step of the Suzuki−Miyaura reaction, the transmetalation of the organoboron compound to form organopalladium species (Scheme 2).[7] Interestingly, in both organic and organometallic precedents, quaternary anionic boron species are the actual alkyl/aryl group donor. For example, transmetalation from boron to palladium in the Sukuzi−Miyaura reaction is typically promoted by adding bases to form a quaternary borate anion (Scheme 2, bottom).[6a,8,9] Since the B−C bond cleavage in Scheme 1 requires no added base, and occurs in noncoordinating solvents, we were curious to learn whether this reaction is mechanistically distinct from the palladium reaction, possibly leading to insights on strategies for milder cross-coupling reactions.

Few boron alkylations of any sort are understood in great mechanistic detail.[10] Below, we describe kinetic studies that give insight into the mechanism of this transformation. The hydridoborate product also undergoes an interesting reaction with hydrazine to cleave the N−N bond to yield a diaminoborate complex.

Scheme 3

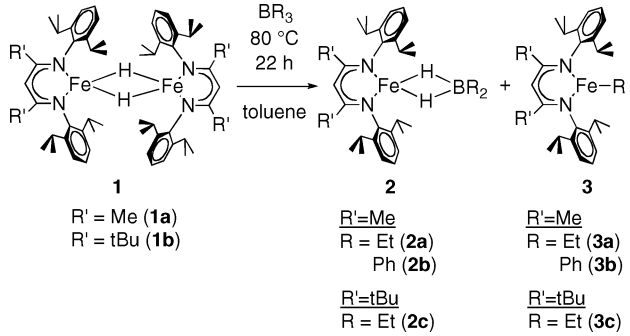

Results and Discussion

Formation of the Dihydridoborate Complex from $L^RFe(\mu\text{-}H)_2FeL^R$ and BEt_3. Reaction of the iron hydride dimers $L^RFe(\mu\text{-}H)_2FeL^R$ (L^R = β-diketiminate ligands shown in Figure 1; **1a** with R = Me and **1b** with R = ^{t}Bu) with 1 molar equiv of BR_3 (R = Et, Ph) in toluene at 80 °C for 22 h leads to an equimolar mixture of a four-coordinate hydridoborate complex, $L^RFe(\mu\text{-}H)_2BR'_2$ (R = Me, R′ = Et **2a** or Ph **2b**; R = ^{t}Bu, R′ = Et **2c**), and an iron alkyl complex L^RFeR' (R = Me, R′ = Et **3a** or Ph **3b**; R = ^{t}Bu, R′ = Et **3c**).[11] These reactions are shown in Scheme 3. Reaction of **1a** with $B(OEt)_3$ and $B(iBu)_3$ gave multiple unidentified products, and these reactions were not pursued further.

The alkyliron compounds **3a** and **3c** were identified by comparison to their known ^{1}H NMR spectra (they can be prepared independently from $[L^RFeCl]_n$ (n = 1 or 2) and Grignard reagents).[12] The new complex $L^{Me}FePh$ (**3b**) was previously unknown, and so it was generated from the reaction of $[L^{Me}Fe(\mu\text{-}Cl)_2FeL^{Me}]$ with PhMgCl. Its spectroscopic features and X-ray crystal structure (see Experimental Section for spectroscopy and Supporting Information for solid-state structure) are analogous to those for the three-coordinate alkyl complexes. The ^{1}H NMR spectrum of independently prepared **3b** verifies that it is identical to one of the products from reaction of **1a** and BPh_3.

The new (dihydridoborate)iron(II) complexes **2a**, **2b**, and **2c** were isolated in 59−72% yield after fractional crystallization away from the iron(II) alkyl/aryl complexes. The reaction of **1a** with BEt_3 was very clean: **1a**, **2a**, and **3a** are the only compounds observed in the ^{1}H NMR spectra of the reaction mixture. In the other reactions, there were a few unidentified paramagnetic peaks in the crude mixtures, representing side products that were removed by crystallization. Each dihydridoborate complex exhibits a magnetic moment of 4.0(1) to 5.7(1) μ_B in C_6D_6 solution, indicating a high-spin iron(II) center (S = 2). Each ^{1}H NMR spectrum covers an extremely wide range from 100 to −310 ppm, with large chemical shift dispersion as a result of the paramagnetic iron ion. The proton resonances were generally assigned from the relative integrations (see Experimental Section). The six-proton peaks for the BEt_2 group and the L^{Me} backbone could be distinguished because the ^{1}H NMR spectra of $L^{Me}Fe(\mu\text{-}H)_2BEt_2$ and $L^{tBu}Fe(\mu\text{-}H)_2BEt_2$ differ only by the six-proton resonance in the L^{Me} compound and the 18-proton resonance in the L^{tBu} compound. The bridging hydride protons are not observed because of fast relaxation.

(7) (a) Miyaura, N.; Suzuki, A. *Chem. Rev.* **1995**, *95*, 2457−83. (b) Chemler, S. R.; Trauner, D.; Danishefsky, S. J. *Angew. Chem., Int. Ed.* **2001**, *40*, 4544−4568. (c) Hayashi, H.; Yamasaki, K. *Chem. Rev.* **2003**, *103*, 2829−2844.

(8) (a) Onak, T. *Organoborane Chemistry*; Academic: New York, 1975. (b) Mikhailov, B. M.; Bubnov, Y. N. *Organoboron Compounds in Organic Synthesis;* Hanvood Academic Publishers: Amsterdam, 1983. (c) Pelter, A.; Smith, K.; Brown, H. C. *Borane Reagents*; Academic: New York, 1988.

(9) BEt_4^- has been used as an ethyl source for the synthesis of organometallics like tetraethyllead: (a) Honeycutt, J. B.; Riddle, J. M. *J. Am. Chem. Soc.* **1961**, *83*, 369−373. (b) Fischer, R.; Rapsomanikis, S.; Andreae, M. R. *Anal. Chem.* **1993**, *65*, 763−766. (c) Rapsomanikis, S. *Analyst* **2004**, *119*, 1429−1439.

(10) (a) Miyaura, N. *J. Organomet. Chem.* **2002**, *653*, 54−57. (b) Zhao, P.; Incarvito, C. D.; Hartwig, J. F. *J. Am. Chem. Soc.* **2007**, *129*, 1876−1877.

(11) Identical product mixtures are obtained when $[L^RFeCl]_n$ (n = 1 or 2) is stirred with $KBHEt_3$ for more than 15 h.

(12) Vela, J.; Vaddadi, S.; Cundari, T. R.; Smith, J. M.; Gregory, E. A.; Lachicotte, R. J.; Flaschenriem, C. J.; Holland, P. L. *Organometallics* **2004**, *23*, 5226−5239.

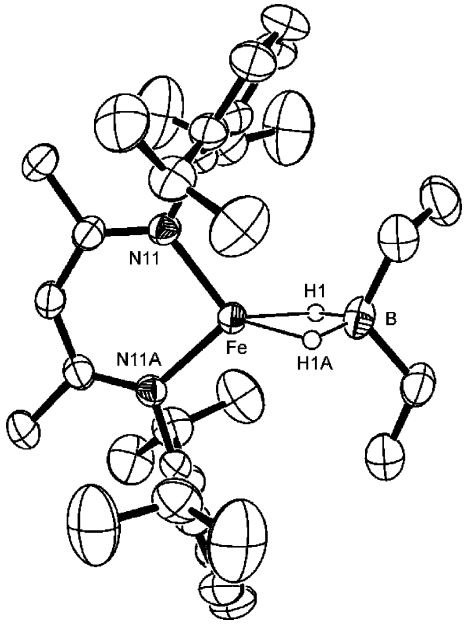

Figure 2. Thermal ellipsoid plot of the molecular structure of $L^{Me}Fe(\mu\text{-}H)_2BEt_2$ (**2a**). A crystallographic C_2 axis passes through Fe and B. Other crystallographic data are in the Supporting Information.

Table 1. Important Bond Distances and Angles for Dihydridoborate Complexes in This Work

complex	Fe−H (Å)	B−H (Å)	Fe−B (Å)
$L^{Me}Fe(\mu\text{-}H)_2BEt_2$ (**2a**)	1.74(2)	1.35(2)	2.237(3)
$L^{Me}Fe(\mu\text{-}H)_2BPh_2$ (**2b**)	1.72(2), 1.72(2)	1.28(2), 1.19(2)	2.239(2)
$L^{tBu}Fe(\mu\text{-}H)_2BEt_2$ (**2c**)	1.74(2), 1.73(2)	1.26(2), 1.21(2)	2.232(1)

A single crystal of each iron dihydridoborate complex was grown from pentane. The solid-state structure of **2a** is shown in Figure 2 as an example, and others may be found in the Supporting Information. The bridging hydride ions were located and refined with an isotropic thermal parameter in each structure (the two hydrides are crystallographically distinct, except in the case of $L^{Me}Fe(\mu\text{-}H)_2BEt_2$, where the hydride positions are related by a C_2 axis). Including the two Fe−H bonds, each iron center has a pseudotetrahedral geometry with a Fe−H distance of about 1.7 Å (Table 1). Although the Fe···B distances are relatively short (ca. 2.24 Å), we do not postulate any direct Fe−B bonding interaction because the two atoms are held in proximity by the bridging hydride.[13] The B−H distances range from 1.19(2) to 1.35(2) Å, which is comparable to the average M−H−B distance of 1.24 Å in the Cambridge Structural Database.

The formation of **2** and **3** is the result of an interesting B−C bond cleavage. Previous examples of B−C cleavage are most often from nucleophilic borates, rather than from boranes.[14] In complexes with covalently bound hydridoborate ligands, $BH_nR_{4-n}^-$ ($n = 1-4$, R = H or alkyl) complexes are much less common than borohydride (BH_4^-) complexes.[15] Known examples of MH_2BR_2 complexes typically come from double metathesis reactions of a metal chloride complex with an alkali metal salt of H_2BR_2 ($R_2 = H_2$,[16] C_5H_{10}, C_8H_{14},[17] and Et_2[15b,18]). In some literature cases, the $H_2BEt_2^-$ group was present from impurities in commercial $HBEt_3^-$.[15b,18,19] Here, the hydridoborate product is formed from cleavage of the B−C bond of a trialkylborane, and *not* from a dihydridoborate impurity in the starting material (see below).

Table 2. Effect of [BEt_3] on Observed Rate Constant

	initial concentrations (mM)		observed rate constant
entry	**1**	BEt_3	k_{obs} (s^{-1})
1	6.4	64.8	$2.2(4) \times 10^{-3}$
2	6.4	129.6	$4.7(2) \times 10^{-3}$
3	6.4	259.0	$9.4(2) \times 10^{-3}$

Reaction of $L^{Me}Fe(\mu\text{-}H)_2FeL^{Me}$ with BR_3: Rate Law and Activation Parameters. We used the reaction of $L^{Me}Fe(\mu\text{-}H)_2FeL^{Me}$ (**1a**) with BEt_3 as the subject of kinetic studies because of the simple ^1H NMR spectra of the starting material and the exceptionally clean reaction. Using an internal integration standard ($L^{tBu}FeCl$) in a sealed capillary, we verified that the spectroscopic yields of products are 95% and 99% for $L^{Me}Fe(\mu\text{-}H)_2BEt_2$ (**2a**) and $L^{Me}FeEt$ (**3a**), respectively. In the kinetic experiments, various amounts of **1a** and BEt_3 (>10 equiv relative to **1a**) were mixed in C_6D_6 and held at various temperatures between 6.5 and 59.7 °C. Complexes **2a** and **3a** were the only products observed by ^1H NMR spectroscopy. The integrations of the peaks at 13 (**1a**), 17 (**2a**), and −11 ppm (**3a**) were followed as a function of time and invariably showed exponential decays. The rate constant was independent of [Fe] when a drop of liquid mercury was added to the reaction mixtures. Without the mercury, we observed a slight decrease in k_{obs} from $3.97(7) \times 10^{-3}$ s^{-1} to $2.51(2) \times 10^{-3}$ s^{-1} with an increase of [**1a**] from 11.1 mM to 42.3 mM. With added Hg^0, the derived k_{obs} showed no clear trend when changing [**1a**] from 20 mM to 40 mM. Therefore, subsequent trials were run with a drop of mercury, which presumably amalgamates trace metallic iron.

For consistency, the following use exclusively the rate constants derived from following the decrease of **1a** (Table 2). The rate has a first-order dependence on [**1a**] (as evident from its exponential decay and the constancy of the rate constant upon

(13) Mehn, M. P.; Brown, S. D.; Paine, T. K.; Brennessel, W. W.; Cramer, C. J.; Peters, J. C.; Que, L., Jr. *Dalton* **2006**, 1347−1351.

(14) Examples of stoichiometric B−C bond cleavage by transition metals: (a) Sacconi, L.; Dapporto, P.; Stoppioni, P. *Inorg. Chem.* **1976**, *15*, 325−329. (b) Siegmann, K.; Pregosin, P. S.; Venanzi, L. M. *Organometallics* **1989**, *8*, 2659−2664. (c) Thaler, E. G.; Caulton, K. G. *Organometallics* **1990**, *9*, 1871−1876. (d) Aresta, M.; Quaranta, E.; Tommasi, I.; Derien, S.; Dunach, E. *Organometallics* **1995**, *14*, 3349−3356. (e) Spence, R. E.; Piers, W. E.; Sun, Y.; Parvez, M.; MacGillivray, L. R.; Zaworotko, M. J. *Organometallics* **1998**, *17*, 2459−2469. (f) Lee, L. W. M.; Piers, W. E.; Elsegood, M. R. J.; Clegg, W.; Parvez, M. *Organometallics* **1999**, *18*, 2947−2949. (g) Plečnik, C. E.; Liu, F.-C.; Liu, S.; Liu, J.; Meyers, E. A.; Shore, S. G. *Organometallics* **2001**, *20*, 3599−3606. (h) Schebler, P. J.; Mandimutsira, B. S.; Riordan, C. G.; Liable-Sands, L. M.; Incarvito, C. D.; Rheingold, A. L. *J. Am. Chem. Soc.* **2001**, *123*, 331−332. (i) Hayes, P. G.; Piers, W. E.; Parvez, M. *Organometallics* **2005**, *24*, 1173−1183.

(15) (a) Marks, T. J.; Kolb, J. R. *Chem. Rev.* **1977**, *77*, 263−93. (b) Ghilardi, C. A.; Innocenti, P.; Midollini, S.; Orlandini, A. *J. Organomet. Chem.* ***1982***, *231*, C78−C80. (c) Ghilardi, C. A.; Innocenti, P.; Midollini, S.; Orlandini, A. *J. Chem. Soc., Dalton Trans.* **1985**, 605−9. (d) Jia, G.; Lough, A. J.; Morris, R. H. *J. Organomet. Chem.* **1993**, *461*, 147−56.

(16) Kandiah, M.; McGrady, G. S.; Decken, A.; Sirsch, P. *Inorg. Chem.* **2005**, *44*, 8650−8652.

(17) (a) Liu, F. C.; Plecnik, C. E.; Liu, S.; Liu, J.; Meyers, E. A.; Shore, S. G. *J. Organomet. Chem.* **2001**, *627*, 109−120. (b) Liu, F.-C.; Chen, J.-H.; Chen, S.-C.; Chen, K.-Y.; Lee, G.-H.; Peng, S.-M. *J. Organomet. Chem.* **2005**, *690*, 291−300.

(18) (a) Fryzuk, M. D.; Lloyd, B. R.; Clentsmith, G. K. B.; Rettig, S. J. *J. Am. Chem. Soc.* **1994**, *116*, 3804−3812. (b) Galler, J. L.; Good-child, S.; Gould, J.; McDonald, R.; Sella, A. *Polyhedron* **2004**, *23*, 253−262. (c) Crestani, M. G.; Munoz-Hernandez, M.; Arevalo, A.; Acosta-Ramirez, A.; García, J. J. *J. Am. Chem. Soc.* **2005**, *127*, 18066−18073.

(19) Selected examples of hydridoborate complexes formed from transition metal hydride complexes: (a) Baker, R. T.; Ovenall, D. W.; Harlow, R. L.; Westcott, S. A.; Taylor, N. J.; Marder, T. B. *Organometallics* **1990**, *9*, 3028−3030. (b) Baker, R. T.; Calabrese, J. C.; Westcott, S. A.; Marder, T. B. *J. Am. Chem. Soc.* **1995**, *117*, 8777−8784. (c) Essalah, K.; Barthelat, J.-C.; Montiel, V.; Lachaize, S.; Donnadieu, B.; Chaudret, B.; Sabo-Etienne, S. *J. Organomet. Chem.* **2003**, *680*, 182−187. (d) Westcott, S. A.; Marder, T. B.; Baker, R. T.; Harlow, R. L.; Calabrese, J. C.; Lam, K. C.; Lin, Z. *Polyhedron* **2004**, *23*, 2665−2677.

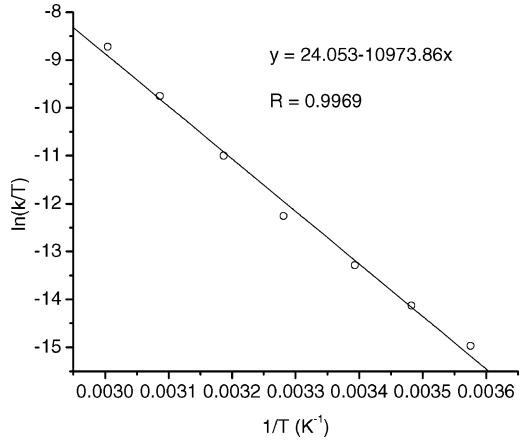

Figure 3. Eyring plot for the reaction of **1a** + BEt_3 to give **2a** and **3a**.

Table 3. Effect of [1a] on Observed Rate Constant[a]

entry	initial concentration (mM) **1a**	initial concentration (mM) BEt_3	observed rate constant k_{obs} (s^{-1})
1	11.6	418.8	$6.58(4) \times 10^{-3}$
2	20.8	418.8	$4.59(2) \times 10^{-3}$
3	30.8	418.8	$4.52(4) \times 10^{-3}$
4	41.6	418.8	$4.27(8) \times 10^{-3}$

[a] For the effect of changes in [**1a**] in the absence of mercury, see the Supporting Information.

Table 4. Rate Constants with Variation of R Groups on the Diketiminate and Borane[a]

iron hydride reagent	BR_3 reagent	pseudo-first-order rate constant k_{obs} (s^{-1})
$L^{Me}Fe(\mu\text{-H})_2FeL^{Me}$ (**1a**)	BEt_3	$3.09(2) \times 10^{-3}$
$L^{Me}Fe(\mu\text{-H})_2FeL^{Me}$ (**1a**)	BPh_3	$8.91(5) \times 10^{-3}$
$L^{tBu}Fe(\mu\text{-H})_2FeL^{tBu}$ (**1b**)	BEt_3	$4.8(2) \times 10^{-3}$

[a] $[BR_3] = 0.419$ M, $[L^RFe(\mu\text{-H})_2FeL^R] = 26$ mM, $T = 40$ °C.

variation of [**1a**]) and a first-order dependence on [BEt_3] (from the linear dependence of the pseudo-first-order rate constant on BEt_3 concentration). Therefore, the rate law is

$$\text{rate} = -\text{d}[\mathbf{1a}]/\text{d}t = k[\mathbf{1a}][BEt_3] \quad (3)$$

The second-order rate constant at room temperature (21.5 °C) was $4.9(1) \times 10^{-4}$ M^{-1} s^{-1}. Activation parameters were calculated from an Eyring plot of second-order rate constants from 6.5 to 59.7 °C (Figure 3), giving $\Delta H^{\ddagger} = 21.8 \pm 0.8$ kcal·mol^{-1} and $\Delta S^{\ddagger} = -1 \pm 2$ eu.[20]

Table 4 shows that varying the steric demands of the diketiminate ligand and BR_3 gives rate constants of the same magnitude, which slightly *increase* with a larger borane (BPh_3) or diketiminate ligand (L^{tBu}). Therefore, there is only a small steric influence on the reaction rate.

Finally, the reaction of **1a** with BEt_3 was repeated in different polar solvents (75% *o*-difluorobenzene/25% C_6D_6 or THF-d_8). We observed a small increase in rate constant using THF, but no increase in a more polar mixture of *o*-difluorobenzene and benzene (Table 5). The similarities in rate with a more polar solvent mixture suggests that charged species are not formed in the rate-limiting transition state (see below). The rate increase in THF may be from coordination of THF to intermediates, but the nature of this interaction was not queried further.

(20) Activation parameters derived from experiments without Hg^0 gave similar values of $\Delta H^{\ddagger} = 21.6 \pm 0.7$ kcal/mol and $\Delta S^{\ddagger} = 2.3 \pm 0.6$ eu. This suggests that the reaction profile is the same in the presence of Hg^0.

Table 5. Solvent Effect on Rate Constant[a]

solvent	dielectric constant	[BEt_3] (mM)	[**1a**] (mM)	k_{obs} (s^{-1})
C_6D_6	2.25[21]	419	21.1	$3.33(1) \times 10^{-3}$
THF-d_8	7.47[22]	419	23.2	$5.77(5) \times 10^{-3}$
75% *o*-$C_6H_4F_2$ + 25% C_6D_6	11.26[b]	419	24.5	$2.57(3) \times 10^{-3}$

[a] Monitored at 40 °C. These experiments were performed without mercury, and therefore the rate constants differ slightly from those in Table 4. [b] The dielectric constant for the mixed solvent is estimated as the weighted average of 14.26 (pure *o*-$C_6H_4F_2$)[23] and 2.25 (pure C_6D_6).

Scheme 4

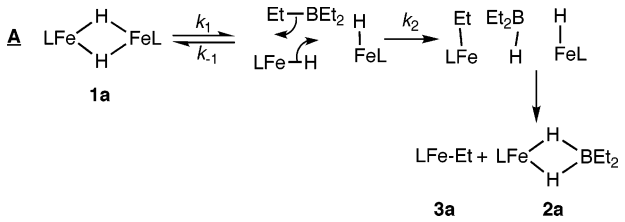

B−C Bond Cleavage: Mechanistic Hypotheses. Several reasonable mechanisms can be proposed for the B−C bond cleavage reaction. We do not consider mechanisms in which BR_3 undergoes β-hydride elimination because the reaction is equally facile with BPh_3, for which β-hydride elimination is impossible. Moreover, independent experiments show that BEt_3 and 1-hexene do not react when heated for 2 h at 80 °C, indicating that borane alkyl groups do not undergo substantial β-hydride elimination under the conditions of the reactions in Scheme 3.

The mechanisms considered here are grouped into categories: dissociation of the iron hydride dimer into monomers before reaction with borane (**A**), concerted Fe−H and B−C cleavage with B−H formation (**B**, **C**, **D**), and formation and disproportionation of a transient iron triethylborohydride species (**E**, **F**).

Dissociation of 1a into Monomer. Mechanism **A** (Scheme 4) illustrates the potential dissociation of the iron hydride dimer as part of the mechanism. A mechanism of this type was strongly implicated in the reaction of $L^{tBu}Fe(\mu\text{-H})_2FeL^{tBu}$ with 3-hexyne, where a zero-order dependence on alkyne concentration indicated an intramolecular rate-limiting step prior to any interaction with alkyne.[4] However, in the reaction with borane described here, hydride dissociation can be ruled out because it does not predict the observed rate law. Mechanism **A** would lead to a zero-order dependence on [BEt_3] if k_1 (dimer dissociation) were rate-limiting or a half order dependence on [**1a**] if k_2 (attack of borane) were rate-limiting.

$$\textbf{A}, k_1 \text{ rate limiting: } \text{rate} = k_1[\mathbf{1a}] \quad (4)$$

$$\textbf{A}, k_2 \text{ rate limiting: } \text{rate} = k_2[\text{LFeH}][BEt_3] = k_2K_{eq}^{1/2}[\mathbf{1a}]^{1/2}[BEt_3] \text{ where } K_{eq} = k_1/k_{-1} \quad (5)$$

The time course of the concentration of **1a** is inconsistent with a half-order dependence of the rate on [**1a**].

Concerted Mechanisms. In mechanism **B** (Scheme 5), **1a** reacts with BEt_3 in an initial rate-limiting step. While the empty boron p-orbital interacts with the bridging hydride, the nucleophilic boron-bound alkyl group simultaneously approaches the iron atom of **1a**. This resembles the "σ-bond metathesis" mechanism that explains C−H activation reactions by d^0 metal

Scheme 5

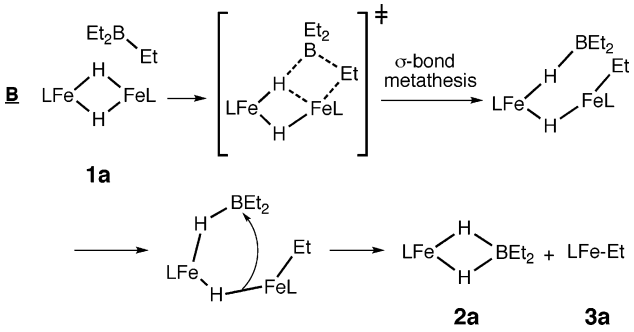

Scheme 6

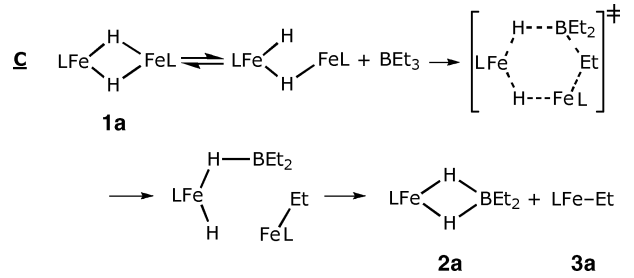

Scheme 7

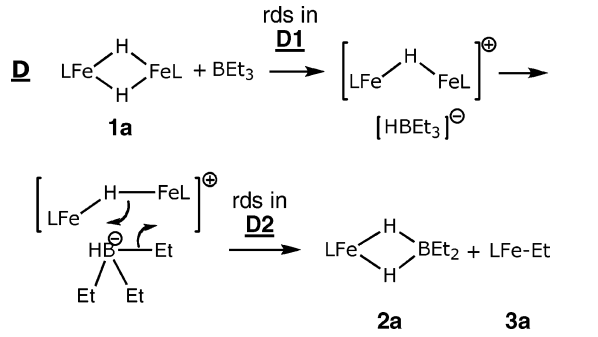

centers.[24] This pathway leads to the observed products after dissociation of a bridging hydride and is the microscopic reverse of the reaction of a ruthenium alkyl complex with catecholborane through a σ-bond metathesis mechanism.[25]

Mechanism **C**, on the other hand, begins with Fe−H bond breaking (Scheme 6). After dissociating *one* of the Fe−H bonds, the "open" isomer leads to a six-membered transition state for a pericyclic reaction. As long as the initial Fe−H opening is rapid and reversible, mechanism **C** agrees with the experimental rate law, rate = k[**1a**][BEt_3].

Mechanism **D** (Scheme 7) starts with rate-limiting abstraction of "H^-" from **1a** by the borane, breaking *two* of the Fe−H bonds and forming free $HBEt_3^-$. Previous researchers have observed alkyl group transfers from a *borate* to a metal center, which is more common compared to group transfer from *borane* species.[14] In analogy, mechanism **D** concludes with transfer of an ethyl group from $HBEt_3^-$ to iron. The ion pair undergoes a σ-bond metathesis to give the final products. Whether the hydride abstraction (**D1**) or the recombination of the ion pair (**D2**) is rate-limiting, the predicted rate law is the same as mechanisms **B** and **C**: a first-order dependence on both [**1a**] and [BEt_3], in accord with the observed rate law.

Notably, each of these mechanisms suffers from inconsistencies with other mechanistic data. First, the entropy of activation near zero is difficult to rationalize in light of the bimolecular transition states in these mechanisms. In order to outweigh the expected large negative entropy change from bringing two molecules together, it is necessary to have a roughly equivalent release of entropy prior to the rate-limiting step. This situation is provided only by mechanisms **C** and **D2**, where the observed rate constant k_{obs} is actually a product of the equilibrium constant for cleavage of one or two Fe−H bond(s) in **1a** (K_{FeH}) and the rate constant for the elementary step consisting of the pericyclic reaction, k_{peri}; $k_{obs} = K_{FeH}k_{peri}$. Therefore $\Delta S^{\ddagger}_{obs} = \Delta S_{FeH} + \Delta S^{\ddagger}_{peri}$. We cannot determine either of these individual entropy values quantitatively, but it is reasonable to postulate that the entropy *increase* from partly opening the crowded dimer structure of **1a** (ΔS_{FeH}) could roughly equal the entropy *decrease* of bringing in the borane or borate to reach the transition state for the pericyclic reaction ($\Delta S^{\ddagger}_{peri}$). Molecular models of the reactants suggest that only an intermediate generated by cleavage of the Fe_2H_2 ring (as in mechanism **C** and **D2**) would have sufficient space for approach of the borane or borate B−C bond.

However, it is difficult to rationalize the similar observed reaction rate between BEt_3 and BPh_3 if mechanism **C** is followed. In the six-membered pericyclic transition state, one of the R groups from the borate sits between the BR_2 fragment and the $L^{Me}Fe$ fragment. Considering the huge hindrance from the β-diketiminate ligand, this conformation is expected to have different steric effects for ethyl and phenyl groups. This argument, as well as the near-zero entropy of activation, makes mechanism **C** less plausible.

In mechanism **D**, we note that an ionic intermediate is formed in or before the rate-limiting transition state. The rate of disappearance of **1a** has very little dependence on solvent polarity, though polar solvents are expected to stabilize transition states in which charge is developing. Therefore, the solvent effect is inconsistent with mechanism **D**.

Borohydride Disproportionation Mechanisms. Commercial solutions of Super-Hydride ($LiHBEt_3$) have been reported to undergo disproportionation to $LiBEt_4$ and $Li[BH_2Et_2]$ at room temperature over long time periods (eq 6).[15b,18b,c,26] The resulting $Li[BH_2Et_2]$ can lead to H_2BEt_2 complexes by metathesis with a metal chloride. In addition, solutions of $LiHBEt_3$·THF are known to react with BEt_3 to give $LiBEt_4$ and $(HBEt_2)_2$, and subsequently $Li[BH_2Et_2]$[18c,26] (eqs 6 and 7).

$$2LiHBEt_3 \rightarrow Li(H_2BEt_2) + LiBEt_4 \quad (6)$$

$$2BEt_3 + 2LiHBEt_3 \rightarrow (HBEt_2)_2 + LiBEt_4 \quad (7)$$

However, the spurious presence of diethylborohydride anions is *not* likely to be involved in the reaction of **1a** with BR_3 for the following reasons. First, our $KHBEt_3$ was prepared in-house from KH and BEt_3 in toluene (eq 8) and stored as a solid. The ^{11}B NMR spectrum of this isolated $KHBEt_3$ in C_6D_6 has a single peak at −16 ppm, with no signs of dihydridoborate or BEt_3 impurities. The ^{11}B NMR spectrum of $KHBEt_3$ did not show

(21) Nath, J.; Tripathi, A. D. *J. Chem. Soc., Faraday Trans.* **1984**, 1517−1524.
(22) Laurence, C.; Nicolet, P.; Dalati, M. T.; Abboud, J. M.; Notario, R. *J. Phys. Chem.* **1994**, *98*, 5807−5816.
(23) Szulejko, J. E.; Mcmahon, T. B. *J. Am. Chem. Soc.* **1993**, *115*, 7839−7848.
(24) (a) Thompson, M. E.; Baxter, S. M.; Bulls, A. R.; Burger, B. J.; Nolan, M. C.; Santarsiero, B. D.; Schaefer, W. P.; Bercaw, J. E. *J. Am. Chem. Soc.* **1987**, *109*, 203−19. (b) Cundari, T. R. *J. Am. Chem. Soc.* **1994**, *116*, 340−347.
(25) Hartwig, J. F.; Bhandari, S.; Rablen, P. R. *J. Am. Chem. Soc.* **1994**, *116*, 1839−1844.
(26) Smith, G.; Cole-Hamilton, D. J.; Thornton-Pett, M.; Hursthouse, M. B. *J. Chem. Soc., Dalton Trans.* **1983**, 2501−2507.

Scheme 8

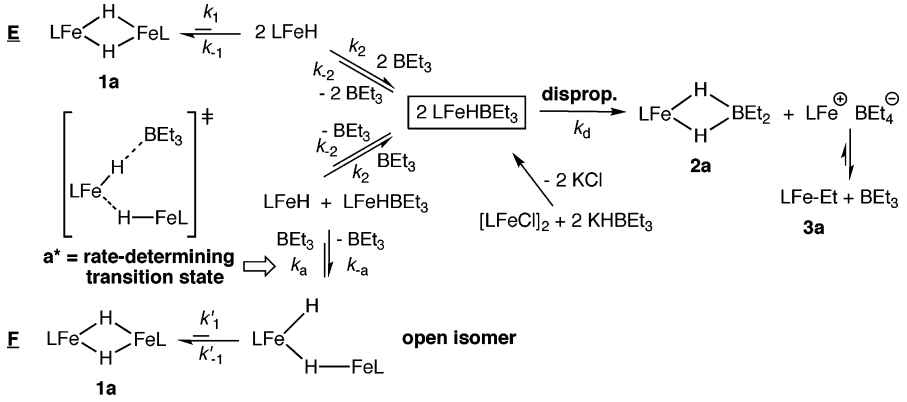

any change when heated to 80 °C for 2 h in benzene-d_6 (mimicking the conditions of our kinetic experiments). An even more convincing piece of evidence is our ability to synthesize $L^{Me}FeH_2BEt_2$ from **1a** and BEt_3, a reaction in which $KHBEt_3$ is not present. Therefore, the presence of potassium diethylborohydride in our reaction is unlikely, and hydridoborate salts do not need to be added for **2a** and **3a** to be formed.

It is still necessary to consider the transient formation of trialkylborohydride species later in the pathway. For example, the first step of the reaction might resemble the reaction of alkali metal hydrides with triethylborane[27] (eq 8).

$$KH + BEt_3 \rightarrow KHBEt_3 \tag{8}$$

The analogous reaction at iron would involve a nucleophilic attack of an iron hydride species on BEt_3 to form a transient iron triethylborohydride complex, $L^{Me}Fe(HBEt_3)$ (center of Scheme 8). Attack could be from the monomer (mechanism **E**) or from a dimer with one Fe−H bond opened (mechanism **F**). Because $L^{Me}Fe(HBEt_3)$ is the presumed intermediate in the reaction of $L^{Me}FeCl$ and $KHBEt_3$ to form $L^{Me}Fe(\mu\text{-}H)_2FeL^{Me}$ + KCl + BEt_3 (eq 1, above), steps preceding the formation of this intermediate are assumed to be reversible (Scheme 8).

Since $L^{Me}Fe(HBEt_3)$ is not observed by NMR spectroscopy during any reaction, this intermediate must be consumed very quickly (k_d and k_2 are large). Assuming that $L^{Me}Fe(HBEt_3)$ is an intermediate on the way to $[L^{Me}Fe(\mu\text{-}H)_2FeL^{Me}]_2$ in eq 1, then k_{-2} and k_{-1} in mechanism **E** or **F** must be larger than k_d (or else **1a** could not be isolated in the reaction of $[L^{Me}FeCl]_2$ and $KHBEt_3$). Therefore k_1, k_2, k'_1, or k_a is rate-limiting. In other words, the rate-determining step (RDS) must happen before the formation of $L^{Me}Fe(HBEt_3)$.

Interestingly, these different rate-limiting steps give three distinct rate laws.

E if RDS is k_1,

$$\text{rate} = k_1[\mathbf{1a}] \tag{9}$$

if RDS is k_2,

$$\text{rate} = k_2K_{eq}^{1/2}[\mathbf{1a}]^{1/2}[BEt_3] \text{ where } K_{eq} = k_1/k_{-1} \tag{10}$$

Mechanism **E** predicts a zero-order dependence on $[BEt_3]$ if k_1 is the RDS or a half-order dependence on [**1a**] if k_2 is the RDS (eq 10). Neither situation agrees with the observed rate law.

F if RDS is k'_1,

$$\text{rate} = k'_1[\mathbf{1a}] \tag{11}$$

if RDS is k_a,

$$\text{rate} = k_aK'_{eq}[\mathbf{1a}][BEt_3] \text{ where } K'_{eq} = k'_1/k'_{-1} \tag{12}$$

In mechanism **F** with k_a as the slow step, the predicted rate law matches that observed experimentally. As shown in Scheme 8, the hydride dimer first opens across *only one* Fe−H bond to form an isomer with one terminal hydride and one bridging hydride. This step must be rapid and reversible. The open isomer of the hydride dimer reacts with one molecule of BEt_3, going through transition state **a*** to give $L^{Me}FeHBEt_3$ and $L^{Me}FeH$. The $L^{Me}FeH$ monomer rapidly reacts with another molecule of BEt_3 to form a second equivalent of $L^{Me}FeHBEt_3$. The two $L^{Me}FeHBEt_3$ species then undergo disproportionation to give the final products.

Mechanism **F** rationalizes the near-zero value for the entropy of activation, because the transition state **a*** involves the dissociation of one Fe−H bond and the formation of one B−H bond. As such, it bears a resemblance to the transition state for an interchange mechanism for substitution at a transition-metal complex (the intermediate category between associative and dissociative substitution reactions). For I_a or I_d mechanisms, values of $\Delta S^{\ddagger}$ near zero are common.[28]

Mechanism **F** is also consistent with other mechanistic data. With the opening of one iron−hydride bond, the β-diketiminate has more space to avoid steric interactions with the borane R group. This explains the similar observed reaction rate for BEt_3 and BPh_3. Finally, there are no ionic intermediates prior to the rate-determining step, which agrees with the lack of a solvent polarity effect during the reaction. On the basis of the above analysis, mechanism **F** is the one most consistent with all experimental data.

Because the key disproportionation step (to the right of $L^{Me}Fe(HBEt_3)$ in Scheme 8) lies after the rate-limiting step, kinetic data are not useful in elucidating its characteristics. Therefore, we endeavored to independently synthesize $L^{Me}Fe^{+}BEt_4^{-}$, the putative intermediate in the reaction.[29] First, reaction of $[L^{Me}FeCl]_2$ and $NaBEt_4$ in Et_2O leads cleanly to the formation of $L^{Me}FeEt$, as observed by ^1H NMR spectroscopy. Also, $L^{Me}FeEt$ does not react with BEt_3 even at 120 °C. This is a thermodynamic phenomenon rather than a kinetic barrier,

(27) Brown, H. C.; Krishnamurthy, S.; Hubbard, J. L. *J. Am. Chem. Soc.* **1978**, *100*, 3343−3349.

(28) Wilkins, R. G. *Kinetics and Mechanism of Reactions of Transition Metal Complexes*; VCH: New York, 1991.

(29) $L^{tBu}Fe(OEt_2)^{+}BAr^{F}_4{}^{-}$ has been reported: Gregory, E. A.; Lachicotte, R. J.; Holland, P. L. *Organometallics* **2005**, *24*, 1803−1805.

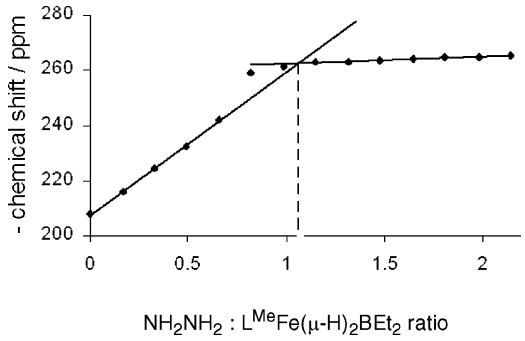

Figure 4. Titration curve , using the chemical shift of the ^{1}H NMR resonance near −260 ppm.

because heating $L^{Me}FePh$ to 80 °C for 3 h with 1 equiv of BEt_3 gives a mixture of $L^{Me}FePh$ and $L^{Me}FeEt$. These experiments strongly suggest that transient $L^{Me}Fe^+BR_4^-$ species are unstable with respect to dissociation of borane, as required in the last step of mechanism **F**. In benzene, the ionic species may exist as a contact ion pair or as a tight ion pair, analogous to a crystallographically characterized tight ion pair between $L^{Me}Fe^+$ and (benzyl)$B(C_6F_5)_3^-$.[30]

*In summary, the available kinetic and mechanistic evidence are most consistent with mechanism **F**, in which a transient ring-opened isomer of **1a** reacts with BR_3 to give $LFeHBR_3$, which converts into the iron dihydridoborate and iron alkyl products through the ionic intermediate $LFeBR_4$.*

$L^{Me}Fe(\mu\text{-}H)_2BEt_2$ Reactivity with Hydrazine: N−N Bond Cleavage. Exploration of the reactivity of the dihydridoborate complex $L^{Me}Fe(\mu\text{-}H)_2BEt_2$ (**2a**) has shown an interesting series of reactions upon the addition of hydrazine. At room temperature, complex **2a** reacts rapidly with H_2NNH_2 to give a hydrazine adduct, $L^{Me}Fe(\eta^1\text{-}H_2NNH_2)(\mu\text{-}H)_2BEt_2$ (**4**), isolated in 90% yield. Titration of hydrazine into a solution of **2a** gave solutions with ^{1}H NMR spectra similar to **2a** but variable chemical shifts, showing that the bound hydrazine is in rapid exchange with free hydrazine. Proton NMR resonances for the N-bound protons are not seen because of their proximity to the paramagnetic metal center.

The binding stoichiometry in solution can be determined by adding small aliquots of hydrazine to **2a** and measuring the change in the ^{1}H NMR spectrum after each addition. The chemical shift of peaks near −260 and 19 ppm vary depending on the ratio of H_2NNH_2 and **2a** (Figure 4 shows the behavior of the peaks near −260 ppm as an example). The intersection of the initial line (deficiency of hydrazine) and final line (deficiency of **2a**) shows that the two molecules bind in a 1:1 stoichiometry in solution.

In the X-ray crystal structure of **4** (Figure 5), the 1:1 stoichiometry is also evident. The hydrazine ligand binds to the iron atom in a η^1 mode and points toward the diketiminate. The bridging hydrogen atoms were again located in Fourier difference maps, and their positions were refined. The geometry of the five-coordinate iron atom is intermediate between ideal square-pyramidal and trigonal-bipyramidal with $\tau = 0.43$.[31] With the higher coordination number at iron, the Fe−H distances increase to 1.82(2) and 1.91(2) Å, which are about 0.1 Å longer than those in **1**. Accordingly, the H−B distances decrease by

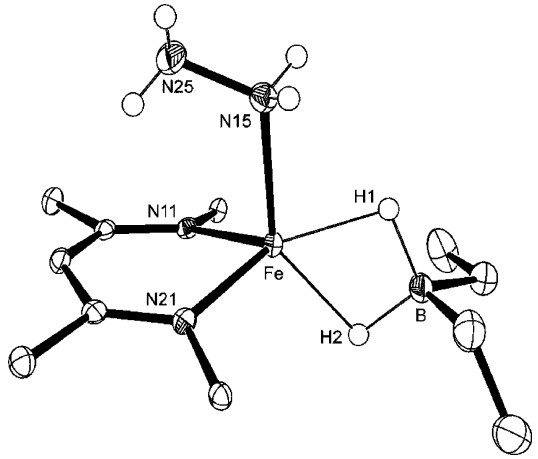

Figure 5. ORTEP diagram of the molecular structure of $L^{Me}Fe(\eta^1\text{-}H_2NNH_2)(\mu\text{-}H)_2BEt_2$ (**4**). Aryl groups and C−H are omitted for clarity. Important bond distances (Å) and angles (deg): Fe−H1 1.91(2), Fe−H2 1.82(2), Fe−N15 2.214(2), B−H1 1.22(2), B−H2 1.22(2), N15−N25 1.441(2), Fe−B 2.350(2), H1−Fe-H2 61.2(9), H1−B−H2 103(1).

Scheme 9

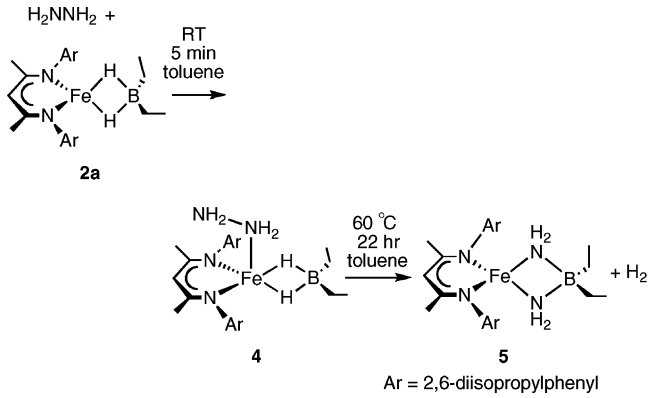

0.12 Å to 1.22(2) Å, comparable to the average value for literature hydridoborate complexes (see Supporting Information). The FTIR spectrum of **4** shows two bands at 3368 and 3333 cm^{-1}, which shifted to 2519 and 2493 cm^{-1} when N_2D_4 was used (calculated from harmonic oscillator: 2460 and 2434 cm^{-1}). Therefore, these are assigned as N−H (N−D) stretching vibrations.[32]

Well-characterized complexes of iron with N_2 and its partial reduction products N_2H_2 and N_2H_4 are rare. A search of the Cambridge Structural Database showed only eight examples of Fe−N_2H_4 species.[32,33] The Fe−N distance in our complex is 2.214(2) Å, which is comparable to the average value of 2.14(3) Å for the known iron−hydrazine adducts. The N−N distance in **4** also agrees well with the average literature value of 1.448(3) Å for bound N_2H_4.

After heating a solution of **4** in toluene at 60 °C for 22 h, the new complex $L^{Me}Fe(\mu\text{-}NH_2)_2BEt_2$ (**5**) can be isolated in 57%

(30) Sciarone, T. J. J.; Meetsma, A.; Hessen, B.; Teuben, J. H. *Chem. Commun.* **2002**, 1580−1581. The equilibrium between $L^{Me}Fe$(benzyl) + $L^{Me}Fe^+[BnB(C_6F_5)_3]^-$ lies to the right.

(31) This parameter is 1 for trigonal bipyramidal, and 0 for square pyramidal. Addison, A. W.; Rao, T. N.; Reedijk, J.; Van Rijn, J.; Verschoor, G. C. *J. Chem. Soc., Dalton Trans.* **1984**, 1349−1356.

(32) In the literature, the number of observed N−H stretching vibrations in Fe−N_2H_4 species varies from two to five. (a) Sellmann, D.; Kreutzer, P.; Huttner, G.; Frank, A. *Z. Naturforsch., B: Chem. Sci.* **1978**, *33B*, 1341−1346. (b) Casey, M. T.; Guinan, P.; Canavan, A.; McCann, M.; Cardin, C.; Kelly, N. B. *Polyhedron* **1991**, *10*, 483−489. (c) Sellmann, D.; Soglowek, W.; Knoch, F.; Ritter, G.; Dengler, J. *Inorg. Chem.* **1992**, *31*, 3711−3717. (d) Sellmann, D.; Shaban, S. Y.; Heinemann, F. W. *Eur. J. Inorg. Chem.* **2004**, 4591−4601.

(33) (a) Sellmann, D.; Blum, N.; Heinemann, F. W. *Z. Naturforsch. B* **2001**, *56*, 581−588. (b) Sellmann, D.; Friedrich, H.; Knoch, F. *Z. Naturforsch. B* **1994**, *49*, 660−664. (c) Goedken, V. L.; Peng, S.-M.; Molin-Norris, J. A.; Park, Y.-A. *J. Am. Chem. Soc.* **1976**, *98*, 8391−400. (d) Rath, S. P.; Olmstead, M. M.; Balch, A. L. *Inorg. Chem.* **2004**, *43*, 6357−6365.

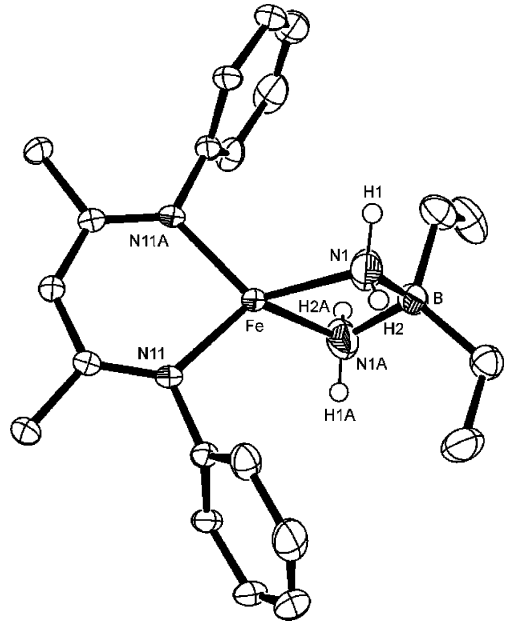

Figure 6. ORTEP diagram of the molecular structure of $L^{Me}Fe(\mu\text{-}NH_2)_2BEt_2$ (**5**) (aryl isopropyl groups and hydrogens are omitted for clarity). There is a crystallographic C_2 axis through Fe and B. Important bond distances (Å) and angles (deg): Fe−N1 2.064(2), Fe−N1A 2.064(1), B−N1 1.571(8), B−N1A 1.577(8), N1−N1A 2.4589(31), N1−Fe−N1A 73.12(9), N1−B−N1A 102.5(3).

yield (Scheme 9). The solid-state structure of **5** is shown in Figure 6. Interestingly, the N−N bond has been cleaved (N···N = 2.459(3) Å) to yield a diaminoborate complex. The IR spectrum shows a *single* N−H stretching band at 3393 cm^{-1}, which shifts to 2494 cm^{-1} in the compound synthesized from N_2D_4. Most complexes containing $M(\mu\text{-}NH_2)_2M$ fragments exhibit two N−H stretching bands between 3100 and 3300 cm^{-1}.[34]

The observation of only one N−H stretching band suggests a possible alternative formulation for **5**, $L^{Me}Fe(\mu\text{-}NH)_2BEt_2$. However, this formally iron(IV) complex seems less likely for several reasons. First, all examples of tetrahedral iron(IV) in the literature are low-spin and supported by strongly donating terminal nitride or imide ligands.[35] The solution magnetic moment of **5** is 4.8(1) μ_B, which is more consistent with a high-spin Fe^{2+} complex (high-spin Fe^{4+} is unlikely). Second, each of the four N-bound H atoms was clearly visible in Fourier maps from the X-ray diffraction experiment and was refined.[36] Finally, the alternative formulation implies that 2 equiv of H_2 are produced in the reaction. Using gas chromatography, we determined that only 1.67 ± 0.03 equiv of H_2 is produced (see Supporting Information for details), inconsistent with the diimidoborate formulation.

Scheme 10

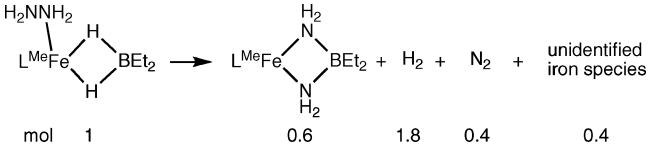

We have no definitive explanation for the observation of H_2 in excess of the amount predicted by the stoichiometry of the reaction in Scheme 9. No substantial amount of H_2 was produced in control experiments where **2a** was heated with hydrazine. However, it is important to note that the spectroscopic yield of **5** is only 60% (from an NMR experiment with internal standard). A substantial amount of a black precipitate is formed along with **5**. It seems possible that the remaining 0.4 equiv of hydrazine is disproportionated to H_2 and N_2 by the iron byproducts, with complete disproportionation giving the limiting stoichiometry in Scheme 10. The rough agreement with the observed H_2 production supports this speculation.

Because **4** has hydrogens in the hydride bridges as well as the bound hydrazine, a final question regards the source of the N−H protons in **5**. Importantly, the synthesis of **5** from N_2D_4 gave a product with no N−H peak and a new N−D peak in the infrared spectrum. This observation indicates that all N−H protons in **5** derive from hydrazine and that the bridging hydrides in **4** are released as H_2 upon heating. Although the unknown nature of some products dissuades us from further mechanistic studies, one can speculate a mechanism where loss of H_2 from **4** generates unsaturation at iron and boron. This would enable coordination of the free lone pair on the bound hydrazine, followed by N−N cleavage to give **5**. However, we stress that other mechanisms are also consistent with the limited data.

A few literature examples report the cleavage of hydrazine N−N bonds with metal-containing clusters, often through formation of bridging NH or NH_2.[37] There are even fewer complexes that cleanly perform this reaction with two or less metals.[38] Here, the Fe−N interactions are reinforced by the low-coordinate environment, which creates strong bonds to electronegative groups, as we have demonstrated previously.[12]

Conclusions

We have discovered an interesting series of borane alkylations/arylations of iron hydride complexes, which give iron hydridoborate products. Kinetic studies have been unusually

(34) (a) Janik, J. F.; Duesler, E. N.; Paine, R. T. *Inorg. Chem.* **1987**, *26*, 4341−4345. (b) Park, S.; Rheingold, A. L.; Roundhill, D. M. *Organometallics* **1991**, *10*, 615−623. (c) Alcock, N. W.; Bergamini, P.; Kemp, T. J.; Pringle, P. G.; Sostero, S.; Traverso, O. *Inorg. Chem.* **1991**, *30*, 1594−1598. (d) Kormos, B. L.; Jegier, J. A.; Ewbank, P. C.; Pernisz, U.; Young, V. G., Jr.; Cramer, C. J.; Gladfelter, W. L. *J. Am. Chem. Soc.* **2005**, *127*, 1493−1503. (e) Stanciu, C.; Hino, S. S.; Stender, M.; Richards, A. F.; Olmstead, M. M.; Power, P. P. *Inorg. Chem.* **2005**, *44*, 2774−2780.

(35) (a) Verma, A. K.; Nazif, T. N.; Achim, C.; Lee, S. C. *J. Am. Chem. Soc.* **2000**, *122*, 11013−11014. (b) Betley, T. A.; Peters, J. C. *J. Am. Chem. Soc.* **2004**, *126*, 6252−6254. (c) Thomas, C. M.; Mankad, N. P.; Peters, J. C. *J. Am. Chem. Soc.* **2006**, *128*, 4956−4957.

(36) In our refinements, the positional parameters and thermal parameter for each hydrogen atom were constrained with respect to the nitrogen atom. If the occupancy of these hydrogen atoms was set to one-half (to consider the possibility of two disordered NH bridges), the thermal parameters for the hydrogen atoms were plainly smaller than those for the parent nitrogen atom, suggesting that insufficient electron density was being modeled and that a full H atom was required in each position.

(37) Selected N−N bond cleavage by metal clusters: (a) Coucouvanis, D. *J. Biol. Inorg. Chem.* **1996**, *1*, 594−600. (b) Shan, H.; Yang, Y.; James, A. J.; Sharp, P. R. *Science* **1997**, *275*, 1460−1462. (c) Verma, A. K.; Lee, S. C. *J. Am. Chem. Soc.* **1999**, *121*, 10838−10839. (d) Seino, H.; Masumori, T.; Hidai, M.; Mizobe, Y. *Organometallics* **2003**, *22*, 3424−3431. (e) Nakajima, Y.; Suzuki, H. *Organometallics* **2003**, *22*, 959−969. (f) Nakajima, Y.; Inagaki, A.; Suzuki, H. *Organometallics* **2004**, *23*, 4040−4046. (g) Takei, I.; Dohki, K.; Kobayashi, K.; Suzuki, T.; Hidai, M. *Inorg. Chem.* **2005**, *44*, 3768−3770.

(38) N−N bond cleavage by mononuclear complexes: (a) Schrock, R. R.; Glassman, T. E.; Vale, M. G.; Kol, M. *J. Am. Chem. Soc.* **1993**, *115*, 1760−1772. (b) Vale, M. G.; Schrock, R. R. *Inorg. Chem.* **1993**, *32*, 2767−2772. (c) Ohki, Y.; Takikawa, Y.; Hatanaka, T.; Tatsumi, K. *Organometallics* **2006**, *25*, 3111−3113. By dinuclear complexes: (d) Schollhammer, P.; Petillon, F. Y.; Poder-Guillou, S.; Saillard, J. Y.; Talarmin, J.; Muir, K. W. *Chem. Commun.* **1996**, 2633−2634. (e) Schollhammer, P.; Guenin, E.; Petillon, F. Y.; Talarmin, J.; Muir, K. W.; Yufit, D. S. *Organometallics* **1998**, *17*, 1922−1924. (f) Petillon, F. Y.; Schollhammer, P.; Talarmin, J.; Muir, K. W. *Inorg. Chem.* **1999**, *38*, 1954−1955. (g) Lin, C.-J.; Hwang, W.-S.; Chiang, M. Y. *J. Organomet. Chem.* **2001**, *640*, 85−92. (g) Shaver, M. P.; Fryzuk, M. D. *J. Am. Chem. Soc.* **2005**, *127*, 500−501.

informative, showing that the most likely mechanism proceeds through attack of a ring-opened iron hydride species on the borane in the rate-determining transition state. In this mechanism, the hydride ligand acts as a nucleophile, apparently activating the borane toward transfer of the R group to iron. In addition, the hydridoborate product of the reaction reacts to cleave the N−N bond of hydrazine, releasing the two bridging hydrides as H_2. The B−C and N−N cleavage reactions demonstrate the ability of low-coordinate iron complexes to perform difficult bond transformations under mild conditions.

Experimental Section

General Considerations. All manipulations were performed under a nitrogen atmosphere using standard Schlenk techniques or in an M. Braun glovebox maintained at or below 1 ppm of O_2 and H_2O. Glassware was dried at 150 °C overnight. ^{1}H NMR spectra were recorded on a Bruker Avance 500 spectrometer (500 MHz) at 22 °C and referenced internally to residual protiated solvent (C_6D_5H at 7.15 ppm). Resonances are broad singlets unless otherwise specified. Infrared spectra (450−4000 cm^{-1}) were recorded on KBr pellet samples in a Shimadzu FTIR spectrophotometer (FTIR-8400S). A total of 32 scans at 2 cm^{-1} resolution were collected in each case. Electronic spectra were recorded between 280 and 1000 nm on a Cary 50 UV−visible spectrophotometer, using screw-cap quartz cuvettes of 1 cm optical path length. Elemental analyses were determined by Desert Analytics (Tucson, AZ). Pentane, tetrahydrofuran (THF), and toluene were purified by passage through activated alumina and "deoxygenizer" columns obtained from Glass Contour Co. (Laguna Beach, CA). Deuterated benzene and THF were dried over CaH_2, then over Na/benzophenone, and then vacuum transferred into a storage container. Before use, an aliquot of each solvent was tested with a drop of sodium benzophenone ketyl in THF solution. Celite was dried overnight at 200 °C under vacuum. Hydrazine, purchased from Aldrich, was dried over KH and vacuum transferred before use. KH, purchased for Aldrich as suspensions in oil, was washed with pentane three times and dried. BEt_3 (1.0 M in hexane) was purchased from Aldrich and used without further purification. The preparation and properties of $[L^{Me}FeCl]_2$, $[L^{Me}FeH]_2$ (**1**), and $KHBEt_3$ were previously reported.[39]

$L^{Me}Fe(\mu\text{-}H)_2BEt_2$ (2a) from 1a. A sample of **1a** (139 mg, 0.147 mmol) was dissolved in 15 mL of toluene. Triethylborane (0.29 mL of a 1.0 M solution in hexane) was added via syringe to the bright red solution. The solution was heated at 70 °C for 14 h. Volatile materials were removed under vacuum, and the residue was extracted with pentane (15 mL), filtered, and concentrated to 5 mL. Crystallization from pentane at −35 °C gave bright red needles (68 mg, 72%).

$L^{Me}Fe(\mu\text{-}H)_2BEt_2$ (2a) from $FeCl_2$. The compound was typically synthesized in one flask from $L^{Me}Li$ and $Fe(THF)_{1.5}Cl_2$ as follows. A Schlenk flask was loaded with a mixture of $L^{Me}Li$ (1.69 g, 3.98 mmol) and $Fe(THF)_{1.5}Cl_2$ (0.94 g, 4.0 mmol) in toluene (50 mL). The mixture was stirred at 80 °C for 22 h. All solvent was removed under vacuum, and a solution of $KHBEt_3$ (0.56 g, 4.0 mmol) in toluene (50 mL) was added. The mixture was heated at 80 °C for 4 h. Volatile materials were removed under vacuum, and the residue was extracted with pentane (100 mL), filtered, and concentrated to 20 mL. Crystallization at −35 °C gave bright red needles (777 mg, 72%). ^{1}H NMR (400 MHz, C_6D_6): 81 (6H, BEt_2 CH_3), 46 (6H, backbone CH_3), 17 (4H), −4 (12H, ^{i}Pr CH_3), −36 (12H, ^{i}Pr CH_3), −40 (4H), −50 (2H, *p*-H), −208 (4H) ppm. (Peaks integrated as 4H could be BEt_2 CH_2, *m*-H, or ^{i}Pr methine. Peaks for the backbone H and bridging H were not observed.) UV−vis (pentane): 299 (ϵ = 27.3 mM^{-1} cm^{-1}), 398 (ϵ = 15.0 mM^{-1} cm^{-1}), 554 (ϵ = 2.9 mM^{-1} cm^{-1}) nm. μ_{eff} (C_6D_6, 25 °C): 5.1(1) μ_B. Anal. Calcd for $C_{33}H_{53}N_2BFe$: C, 72.80; H, 9.81; N, 5.15. Found: C, 73.52; H, 9.52; N, 5.62.

$L^{Me}Fe(\mu\text{-}H)_2BPh_2$ (2b). 1a (127 mg, 0.13 mmol) and triphenylborane (32 mg, 0.13 mmol) were dissolved in 20 mL of toluene. The solution was heated at 80 °C for 18 h. Volatile materials were removed under vacuum, and the residue was extracted with toluene (15 mL), filtered, and concentrated to 5 mL. Crystallization from pentane at −26 °C gave red blocks (56 mg, 67%). ^{1}H NMR (500 MHz, C_6D_6): 78 (6H, backbone CH_3), 32 (4H), 17 (4H+4H), −4 (12H, ^{i}Pr CH_3), −8 (2H), −40 (12H, ^{i}Pr CH_3), −46 (4H), −52 (2H) ppm. (Peaks integrated as 4H could be ^{i}Pr methine, aryl *m*-H, phenyl *o*-H, or phenyl *m*-H. Peaks integrated as 2H could be aryl *p*-H or phenyl *p*-H. Peaks for the backbone H and bridging H were not observed.) UV−vis (toluene): 291 (ϵ = 14.6 mM^{-1} cm^{-1}), 398 (ϵ = 6.3 mM^{-1} cm^{-1}), 567 (ϵ = 1.2 mM^{-1} cm^{-1}) nm. μ_{eff} (C_6D_6, 25 °C): 4.0(1) μ_B. Anal. Calcd for $C_{41}H_{53}BFeN_2$: C, 77.12; H, 8.05; N, 4.39. Found: C, 76.88; H, 7.85; N, 4.38.

$L^{tBu}Fe(\mu\text{-}H)_2BEt_2$ (2c). A Schlenk flask was loaded with a mixture of $L^{tBu}FeCl$ (722 mg, 1.21 mmol) and $KHBEt_3$ (167 mg, 1.21 mmol) in toluene (50 mL). The mixture was stirred at 80 °C for 18 h. Volatile materials were removed under vacuum, and the residue was extracted with pentane (50 mL), filtered, and concentrated to 10 mL. Crystallization at −26 °C gave dark red blocks (224 mg, 59%). ^{1}H NMR (500 MHz, C_6D_6): 71 (6H, BEt_2 CH_3), 42 (1H, backbone), 35 (18H, backbone CH_3), 16 (4H), −13 (12H, ^{i}Pr CH_3), −61 (12H, ^{i}Pr CH_3), −66 (4H), −89 (2H, p-H), −313 (4H) ppm. (Peaks integrated as 4H could be BEt_2 CH_2, *m*-H, or ^{i}Pr methine. Peaks for the bridging H were not observed.) UV−vis (pentane): 333 (ϵ = 9.42 mM^{-1} cm^{-1}), 414 (ϵ = 6.82 mM^{-1} cm^{-1}), 597 (ϵ = 1.27 mM^{-1} cm^{-1}) nm. μ_{eff}(C_6D_6, 25 °C): 5.7(1) μ_B. Anal. Calcd for $C_{39}H_{65}N_2BFe$: C, 74.52; H, 10.42; N, 4.46. Found: C, 74.60; H, 10.20; N, 4.34.

Complexes **3a** and **3c** have been reported in ref 12.

$L^{Me}FePh$ (3b). The compound was typically synthesized in one flask from $L^{Me}Li$ and $FeCl_2(THF)_{1.5}$ as follows. A resealable flask was loaded with a mixture of $L^{Me}Li$ (592 mg, 1.4 mmol) and $FeCl_2(THF)_{1.5}$ (329 mg, 1.4 mmol) in toluene (20 mL). The mixture was stirred at 80 °C for 22 h. Phenylmagnesium chloride (2.0 M in THF, 0.7 mL, 1.4 mmol) was added, and the mixture was stirred for 4 h at room temperature. Solvent was removed under vacuum. The residue was extracted with pentane (20 mL), filtered through Celite, concentrated to 3 mL, and cooled to −45 °C to give bright yellow crystals (487 mg, 63% yield). ^{1}H NMR (C_6D_6, 21 °C): 163 (2H, phenyl *m*-CH), 126 (1H, phenyl *p*-CH), 47 (6H, backbone CH_3), 28 (1H, backbone CH), −10 (4H, *m*-CH), −21 (12H, ^{i}Pr CH_3), −82 (2H, *p*-CH), −118 (4H, ^{i}Pr CH), −125 (12H, ^{i}Pr CH_3). (Phenyl *o*-CH was not observed. Peak assignments were based on integrations and ^{1}H NMR spectra of other known $L^{Me}FeR$ complexes.) UV−vis (pentane): 325 (ϵ = 15.6 mM^{-1} cm^{-1}), 368 (ϵ = 11.4 mM^{-1} cm^{-1}), 494 (ϵ = 1.0 mM^{-1} cm^{-1}) nm. μ_{eff} (C_6D_6, 25 °C): 5.2(1) μ_B. Anal. Calcd for $C_{35}H_{46}N_2Fe$: C, 76.35; H, 8.42; N, 5.09. Found: C, 76.06; H, 8.20; N, 4.99.

$L^{Me}Fe(H_2NNH_2)(\mu\text{-}H)_2BEt_2$ (4). $L^{Me}Fe(\mu\text{-}H)_2BEt_2$ (221 mg, 0.407 mmol) was dissolved in diethyl ether (10 mL). Hydrazine (13 μL, 0.41 mmol) was added via syringe to the bright red solution. The solution was shaken, causing an immediate color change from bright red to orange-pink. The solution was concentrated to 2 mL and cooled to −35 °C to give bright pink-yellow needles of **4** (212 mg, 90%). ^{1}H NMR (400 MHz, C_6D_6): 24 (6H), 19 (4H), 3 (12H, ^{i}Pr CH_3), 1 (6H), −15 (12H, ^{i}Pr CH_3), −24 (4H), −40 (2H, *p*-H), −62 (1H, backbone C−H), −260 (4H) ppm. (Peaks integrated as 4H could be BEt_2 CH_2, *m*-H, or ^{i}Pr methine. Peaks integrated as 6H could be BEt_2, CH_3, or backbone CH_3. Peaks for the bridging

(39) Eckert, N. A.; Smith, J. M.; Lachicotte, R. J.; Holland, P. L. *Inorg. Chem.* **2004**, *43*, 3306−3321. Smith, J. M.; Lachicotte, R. J.; Holland, P. L. *J. Am. Chem. Soc.* **2003**, *125*, 15752−15753. Vela, J.; Smith, J. M.; Yu, Y.; Ketterer, N. A.; Flaschenriem, C. J.; Lachicotte, R. J.; Holland, P. L. *J. Am. Chem. Soc.* **2005**, *127*, 7857−7870.

H and hydrazine H were not observed.) IR (KBr pellet): 3368 cm^{-1}, 3338 cm^{-1} (N−H). UV−vis (pentane): 298 (ϵ = 13.4 mM^{-1} cm^{-1}), 397 (ϵ = 7.5 mM^{-1} cm^{-1}), 552 (ϵ = 1.5 mM^{-1} cm^{-1}) nm. μ_{eff} (C_6D_6, 25 °C): 3.8(1) μ_B. Anal. Calcd for $C_{33}H_{57}N_4BFe$: C, 68.75; H, 9.97; N, 9.72. Found: C, 68.01; H, 8.83; N, 5.70. The bound hydrazine could be removed by extended pumping under vacuum (i.e., 50% of the hydrazine was removed after 26 h at RT), and we suspect that this is the reason for the low nitrogen analysis.

$L^{Me}Fe(\mu\text{-}NH_2)_2BEt_2$ (5). A sample of $L^{Me}Fe(\mu\text{-}H)_2BEt_2$ (201 mg, 0.371 mmol) was dissolved in toluene (15 mL). Hydrazine (14 μL, 0.45 mmol) was added via syringe to the bright red solution. The solution was shaken and then heated at 60 °C for 22 h. Volatile materials were removed under vacuum, and the residue was extracted with pentane (15 mL), filtered, and concentrated to 2 mL. Crystallization from pentane at −35 °C gave brown blocks (121.6 mg, 57%). ^{1}H NMR (500 MHz, C_6D_6): 57 (4H), 33 (6H), 19 (4H), 2 (12H, ^{i}Pr CH_3), −20 (12H, ^{i}Pr CH_3), −35 (4H), −42 (1H, backbone C−H), −49 (2H, *p*-H), −71 (6H) ppm. (Peaks integrated as 4H could be BEt_2 CH_2, *m*-H, or ^{i}Pr methine. Peaks integrated as 6H could be BEt_2, CH_3, or backbone CH_3. Peaks for the bridging NH_2 groups were not observed.) IR (KBr pellet): 3393 cm^{-1} (N−H). UV−vis (pentane): 331 (ϵ = 16.0 mM^{-1} cm^{-1}). μ_{eff} (C_6D_6, 25 °C): 4.8(1) μ_B. Anal. Calcd for $C_{33}H_{55}N_4BFe$: C, 68.99; H, 9.65; N, 9.75. Found: C, 68.68; H, 9.45; N, 9.35.

Kinetic Experiments: Effect of BEt_3. $[L^{Me}FeH]_2$ (16.4 mg, 17.3 mmol) was dissolved in C_6D_6 (2.0 mL). A J. Young NMR tube, which was predried at 180 °C, was loaded with 0.4 mL of the above iron hydride complex solution and 0.14 mL of BEt_3 (1.0 M in hexane) C_6D_6 solution (with various BEt_3 concentrations; see Supporting Information). The NMR tube was placed into the NMR probe, which was equilibrated at the appropriate temperature (typically 319.2 K). After the sample had equilibrated for 2 min, ^{1}H NMR spectra were recorded at preset times using an automated program. After Fourier transform, phasing, calibrating, and integrating each spectrum using MestRec, a plot of normalized [**1a**] (y) versus reaction time (x) was generated. Then these experimental data were fitted into the general, integrated equation $y_0 + A_1 \exp(-x/t_1)$, where y_0, A_1, and t_1 are variables, t_1 being the reciprocal of the first-order rate constant. Origin 6.1 was employed for the data fitting. The error bars on the rate constant came from the least-squares fit to the data.

Kinetic Experiments: Effect of $[L^{Me}FeH]_2$. BEt_3 (1.34 mL, 1.0 M hexane solution) was mixed with C_6D_6 (1.86 mL) and used as a stock solution. A predried J. Young NMR tube was charged with different amounts of **1a** and BEt_3 (0.3 mL of standard solution), with a drop of metallic mercury (see text).

Kinetic Experiments: Activation Parameters. In the range 280−300 K, temperatures in the NMR probe were calibrated using 100% methanol; in the range 300−380 K, 100% ethylene glycol was used for calibrations (Bruker Instruments, VT-Calibration manual). **1a** (73.7 mg, 77.7 mmol) was dissolved in C_6D_6 (1.86 mL), then BEt_3 (1.34 mL, 1.0 M hexane solution) was added to make the reaction solution. For each temperature, 0.3 mL of the reaction solution was injected into a J. Young NMR tube with one drop of metallic mercury. The reaction solution was stored at −35 °C when it was not in use.

Acknowledgment. This work was supported by the NSF (CHE-0134658 to P.L.H.), the NIH (GM-065313 to P.L.H.), and the University of Rochester (Weissberger Fellowship to Y.Y.). P.L.H. acknowledges an A. P. Sloan Fellowship. We thank Jeremy Smith for initial synthetic experiments, William Jones, Thomas Cundari, and Benjamin Dible for helpful discussions, Pingwu Du and Richard Eisenberg for assistance with GC equipment, and Christine Flaschenriem for collecting crystallographic data.

Supporting Information Available: Synthetic, analytical, and kinetic details (PDF) and crystallographic data (CIF). This material is available free of charge via the Internet at http://pubs.acs.org.

OM7003805